PROCEEDINGS REPRINT

Reprinted from

Multilayer and Grazing Incidence X-Ray/EUV Optics for Astronomy and Projection Lithography

19–22 July 1992
San Diego, California

P

Volume 1742

/,', '''
'/,'/ '/'''- '/''/(

Design and Fabrication of the All-Reflecting
H-Lyman α Coronagraph/Polarimeter

Richard B. Hoover
Space Science Laboratory, ES52
NASA/Marshall Space Flight Center, AL 35812

R. Barry Johnson
Optical E.T.C., Inc.
Huntsville, AL 35801

Silvano Fineschi*
Harvard-Smithsonian Center for Astrophysics,
60 Garden St., M/S 50. Cambridge, MA 02138

Arthur B. C. Walker, Jr.
Center for Space Science and Astrophysics
Stanford University, Stanford, CA 94305

Phillip C. Baker
Baker Consulting
Walnut Creek, CA 94305

Muamer Zukic and Jongmin Kim
The University of Alabama in Huntsville
Huntsville, AL 35899

ABSTRACT

We have designed, analyzed, and are now fabricating an All-Reflecting H-Lyman α Coronagraph/Polarimeter for solar research. This new instrument operates in a narrow bandpass centered at λ 1215.7 Å–the neutral hydrogen Lyman α (Ly-α) line. It is shorter and faster than the telescope which produced solar Ly-α images as a part of the MSSTA payload that was launched on May 13, 1991. The Ly-α line is produced and linearly polarized in the solar corona by resonance scattering, and the presence of a magnetic field modifies this polarization according to the Hanle effect. The Lyman α Coronagraph/Polarimeter instrument has been designed to measure coronal magnetic fields by interpreting, via the Hanle effect, the measured linear polarization of the coronal Ly-α line. Ultrasmooth mirrors, polarizers, and filters are being flow-polished for this instrument from CVD silicon carbide substrates. These optical components will be coated using advanced induced transmission and absorption thin film multilayer coatings, to optimize the reflectivity and polarization properties at 1215.7 Å. We describe some of the solar imaging results obtained with the MSSTA Lyman α coronagraph. We also discuss the optical design parameters and fabrication plans for the All-Reflecting H-Lyman α Coronagraph/Polarimeter.

1. INTRODUCTION

At present, coronal magnetic fields can be only indirectly estimated by heavily model-dependent interpretations of radio observations, or by the extrapolation of measured photospheric fields using computational models. We are now developing a coronagraph/polarimeter capable of operating in a narrow bandpass centered on the neutral hydrogen Lyman α (Ly-α) line at 1215.7 Å. This new instrument is designed to derive vector magnetic fields in the inner corona by observing linear polarization by resonant scattering of Ly-α photons in the solar corona. The scientific rationale for this Lyman α Coronagraph/Polarimeter instrument resides in the fact that the dominant process of formation of the coronal Ly-α line is resonant photo-excitation

---

* Also: Dipartimento di Astronomia e Scienza dello Spazio, Università di Firenze, Largo E. Fermi 5, 50125 Firenze (Italy).

of the residual coronal hydrogen by the intense Ly-α chromospheric source, followed by spontaneous decay. Since the illuminating source is anisotropic, and collisional effects are negligible, the Ly-α radiation produced by this resonance scattering mechanism will be linearly polarized. The presence of magnetic fields in the corona modifies the polarization state of this radiation through a process known as the *Hanle effect*. Consequently, determinations of the Stokes parameters of the coronal hydrogen Ly-α radiation by this new instrument may well provide the first direct diagnostics of vector magnetic fields in the solar corona.

The Ly-α Coronagraph/Polarimeter we are developing is a modular, all-reflecting instrument which, for the sake of brevity, we will refer to as the "LyαCoPo." The optical components for the LyαCoPo feature advanced thin-film multilayer coatings, deposited on ultrasmooth, flow-polished mirror substrates, to produce high performance, low-scatter Ly-α mirrors, polarizers, and filters. Many of the mirror fabrication, mounting, assembly, and alignment techniques and methods that were developed for our multilayer x-ray telescopes and microscopes are also being used for the LyαCoPo. In 1987, Walker *et al.*[1,2] obtained the first high resolution soft x-ray and extreme ultraviolet (EUV) images of the Sun using normal incidence multilayer telescopes flown on the Stanford/MSFC/LLNL Rocket X-Ray Spectroheliograph. High resolution full disk and coronal images were obtained on that flight at soft x-ray (44 Å) and EUV (173 Å and 256 Å) wavelengths. The Cassegrain and Herschelian telescopes clearly established the power of single- and double-reflecting multilayer optics and the Wolter-Cassegrain Spectral Slicing Telescope onboard demonstrated the use of multilayer x-ray optics for enhancing the performance of grazing incidence optics.[3] The Cassegrain telescopes recorded 173-Å and 256-Å images on experimental Kodak T-Max 100 film which revealed high resolution details of active regions, loops, and other bright emission regions on the disk simultaneously with faint, low contrast, coronal features. Indeed, the solar images recorded at 173 Å (Fe IX, Fe X) were used to analyze the density structure of a polar coronal plume[1] out to an heliocentric distance r = 1.7 $R_\odot$ (solar radii). More recenty, Walker *et al.*[4,5] have modeled these plumes as miniature helmet streamers with a constant cross-section embedded in a lower density coronal region of open field geometry (i.e., the interplume region). It is important to note that these solar images were produced with doubly reflecting multilayer telescopes using spherical optics with surface smoothness of only ~ 5 Å rms, without a Lyot stop or occulters of any type. Since the solar disk is some 10-100 times brighter than the corona at EUV wavelengths, simultaneously imaging the disk and corona at these wavelengths is easier than at far ultraviolet (FUV) and visible wavelengths, where the brightness ratio is considerably more demanding.

2. THE MSSTA LYMAN-α CORONAGRAPH

On May 13, 1991, we flew a sophisticated solar observatory which was designated the Multi-Spectral Solar Telescope Array (MSSTA). In addition to a re-flight of the 6.3-cm diameter 173-Å Cassegrain telescope from the Stanford/MSFC/LLNL Rocket X-Ray Spectroheliograph, the MSSTA payload included another Cassegrain operating at 211 Å, five soft x-ray/EUV Herschelian telescopes and seven, 12.7-cm diameter Ritchey-Chrétien telescopes coated with multilayers for EUV observations and thin film interference coatings to produce FUV solar images. The Zerodur optics for the Ritchey-Chrétien systems were flow-polished by Baker Consulting to achieve ultrasmooth ($\leq$ 2 Å rms) surfaces.[6,7] The MSSTA flight conclusively demonstrated that coronagraphs using ultrasmooth flow-polished mirrors could image the solar disk and inner corona simultaneously, even at FUV wavelengths where the disk/corona brightness ratio is ~ $10^4 - 10^5$. The MSSTA Ly-α coronagraph used wide latitude, Kodak XUV 100 and Kodak 649 films to obtain high resolution images of the solar disk, while recording the solar corona at Ly-α out to 2 $R_\odot$ from disk center. Hoover *et al.*[8] have shown that the coronal features seen in the digitized and enhanced solar images correlate well with limb features shown on the corrresponding NOAA SESC neutral line drawings. Figure 1 shows (a) the full disk Lyman α image as recorded on the very high resolution but low sensitivity Kodak 649 emulsion and (b) an enlargement of the SW limb, showing spicules, threadlike structures, and prominence features in the inner corona wherein the Hanle effect is highly sensitive.

The limitations of the Ly-α coronal observations were imposed by the frame boundaries of the 70 mm film used and the allowable field of view (as established by the plate scale and film format) of the 3.5 m focal length Ritchey-Chrétien coronagraph. A fast, short focal length, normal incidence multilayer Herschelian telescope operating in the EUV at 193 Å (Fe XII), afforded a wider field of view and was able to record the
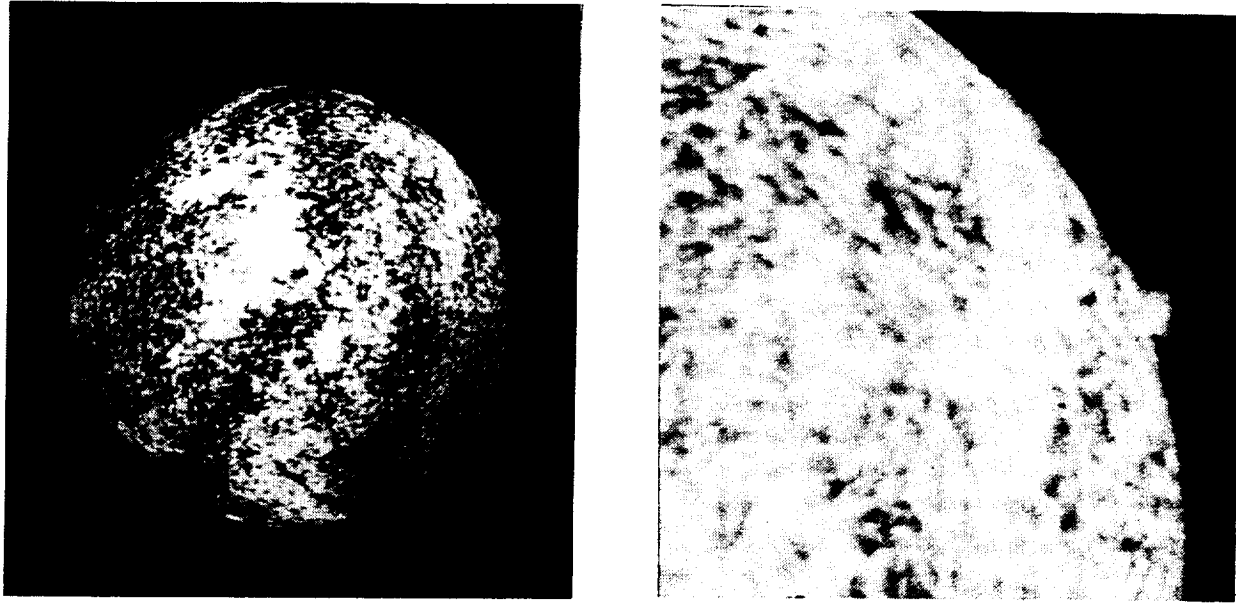
Figure 1a. H-Lyman α image of the solar disk and inner corona as recorded on Kodak 649 film on May 13, 1991, by the Multi-Spectral Solar Telescope Array. **b.** Enlargement of the SW limb to reveal spicules, prominences, and threadlike features in the inner corona.

solar corona out to 4 $R_\odot$ on the high sensitivity XUV 100 photographic emulsion. Clearly, high sensitivity photographic films with very large dynamic range are ideally suited for an imaging solar coronagraph, due to the large brightness range that exists between active regions, flares and the faint structures in coronal holes and the outer corona.[9]

The high resolution images of the solar disk and corona simultaneously achieved by the MSSTA at selected wavelengths in the soft x-ray, EUV, and FUV portions of the electromagnetic spectrum conclusively established that all-reflecting Lyman-α coronagraphs could image the solar disk and corona, without the use of occulters. In the past, white light coronagraphs have typically used high quality refracting optics, occulters, field stops, and baffles to allow the faint coronal emission to be seen in the presence of the vastly brighter solar disk. In white light the solar disk is typically $10^7 - 10^8$ times brighter than the corona, so very low-scatter refractive or reflective optics and optimized stop and baffle configurations are essential. At hydrogen Ly-α the situation is considerably different. The disk is only $10^4 - 10^5$ times brighter than the corona. This lower brightness ratio at Ly-α greatly simplifies stray light rejection problems and permits Ly-α images to be obtained with all-reflecting coronagraphs without the use of an occulter, allowing the solar disk and coronal emissions to be observed simultaneously.

White light coronagraphs (3500 Å to 7000 Å) were flown on OSO-7, Skylab, the Solar Maximum Mission (SMM), and Air Force P-78 satellites.[10,11] All of these coronagraphs were incapable of observing the inner corona since their occulters were at least 50% larger than the solar disk image and obstructed all radiation from the disk and inner corona (i.e., heliocentric distances r $\leq$ 1.5 $R_\odot$). This is precisely the regime wherein the most interesting and exciting magnetic field configurations exist and the magnetic field strength is in the intensity range at which the Ly-α is sensitive via the Hanle effect.[12] Bonnet et al.[13] flew a Ly-α coronagraph (without an occulter) on a rocket in 1979 to produce simultaneous Ly-α images of the disk and corona. Their images revealed intricate coronal structures, spicules, and threadlike features in Ly-α prominences above the limb in the altitude regime which is of high sensitivity for measurements of magnetic fields via the Hanle effect. However, due to the frame boundaries of the 35 mm film, the exposure times, and the limited latitude of the Schumann film they used, observation of the outer Ly-α corona was not possible during that flight.

3. MODULAR LYMAN-α CORONAGRAPH/POLARIMETER

The All-Reflecting Ly-α Coronagraph/Polarimeter instrument we are developing will be capable of simultaneously producing high resolution images of the solar disk and corona. In addition, it will also be capable of determining the state of linear polarization, of the solar Ly-α radiation so as to permit measurements of coronal magnetic fields via the Hanle effect. To optimize the LyαCoPo instrument configuration we have chosen a modular configuration with an Imager Module to which we can attach any one of several candidate Ly-α Polarizer/Filter/Camera modules.

The Imager Module is an aplanatic system comprised of a 2.3-m focal length Ritchey-Chrétien optical system using ultrasmooth hyperboloidal primary and secondary mirrors. The optics will be mounted in mirror cells using a zero outgassing, two part silicone rubber silastic RTV, in a manner such as was used with the MSSTA Ritchey-Chrétien telescopes.[14] The assembled Imager Module optical components will be housed within a filament wound graphite epoxy tube structure of high strength and superb dimensional stability. The Imager Module is designed to have a large back focal distance to accommodate the Ly-α Polarizer/Filter Module.

The Ly-α Polarizer/Filter Modules we are developing for the LyαCoPo are also state-of-the-art components using advanced multilayer thin-film coatings which will be applied to the ultrasmooth, optically flat mirror substrates. For these Ly-α polarizers and filters, we plan to employ optical components using the advanced induced transmision and absorption multilayer coatings which are being developed by Kim *et al.*[15,16] at the University of Alabama in Huntsville (UAH). These novel optical components offer vastly superior polarization and reflectance properties over the more conventional Brewster angle polarizers. The induced transmission and absorption polarizers are very insensitive to small variations of the angle of the incidence for which they are designed to operate. Hence, they function well in non-telecentric systems, such as we have chosen to utilize. Telecentric systems are those in which the entrance pupil and/or the exit pupil is located at infinity.[17] Coronagraph/polarimeter instruments which employ a telecentric mount configuration would prevent the polarizer from being located in a diverging beam. In this case, the variation of angles with which the rays strike the polarizer would be due only to the angular subtense of the solar corona. However, to realize such a telecentric system for the Lyman α Coronagraph/Polarimeter would require the use of additional reflective of refractive optical components at a penalty of increased complexity, greater cost, and reduced system throughput. Refractive optics could also introduce undesired phase shifts and other polarization effects. Fortunately, the induced transmission and absorption polarizers are suffuciently insensitive to the angle of incidence of the radiation[18] and thus telecentric configurations are not required.

The Polarizer/Filter Module will be constructed such that it can be aligned and tested as a compact unit or equipped with a camera and coupled to the Imager Module for test and analysis of the entire system. We have chosen to design, fabricate, and test a single 2.3-m focal length Ritchey-Chrétien Imager Module which will then be utilized in conjunction with any one of the three candidate Polarizer/Filter Modules we plan to fabricate and test. Specifically, we plan to construct:

1. A Polarizer/Filter Module in a single configuration using induced transmission and absorption coatings on ultrasmooth substrates for a single Ly-α polarizer followed by a single Ly-α filter. These components will be designed to operate nominally at 45° angle of incidence, to achieve maximum system throughput at Ly-α, excellent s/p ratio (i.e., polarization efficiency), and low sensitivity to angular convergence of the incident beam (i.e., non-telecentric mount effects).

2. A double Polarizer/Filter Module using two 45° induced transmission and absorption polarizers followed by two 45° induced transmission and absorption filters for superb extinction ratio and very narrow bandpass at Ly-α. This configuration is extremely insensitive to non-telecentric effects and affords vastly superior UV and visible light rejection.

3. A Polarizer/Filter Module with one induced transmission and absorption polarizer (mounted near focus) containing an elliptical "beam scraper" aperture. The very bright image of the solar disk passes through the aperture to be reflected to the camera by the subsequent Ly-α induced transmission and absorption filter. The exterior region of the polarizer reflects the Ly-α coronal image to a separate Ly-α filter and

camera. This minimizes scattered disk radiation and allows different types of photographic emulsions to be employed for the solar disk and coronal images. It should be noted that this configuration preserves vital data concerning disk emissions. This valuable information would be lost with a Gregorian or other optical configuration, which uses an opaque stop situated so as to occult the solar disk and near corona. Optical systems with occulters have been used for almost all previous coronagraph configurations.

These reflecting Ly-α induced transmission and absorption polarizers represent a profound advancement over classic reflecting polarizers operating at the Brewster angle, which always presented a tradeoff between high throughput and high polarization efficiency. (For instance, gold-coated polarizers offer high reflectivity but low polarization efficiency, and crystals such as MgF_2 offer high polarization efficiency but low throughput.) These induced transmission and absorption polarizers represent a completely new class of Ly-α polarizers in that they combine high throughput and high polarization efficiency.

4. OPTICAL CONFIGURATIONS

The Ly-α Coronagraph/Polarimeter instrument is of the Ritchey-Chrétien optical configuration, which is an aplanatic form of the Cassegrain. An aplanat is an optical system in which both coma (to third order, at least) and spherical aberration are absent. Aplanatic telescopes can achieve excellent optical performance over a very wide field of view. The Ritchey-Chrétien system uses a concave hyperboloidal primary and a convex hyperboloidal secondary, as opposed to the aplanatic Gregorian in which a concave secondary is used to refocus the real image formed by the primary optic. The aplanatic Gregorian system is ideal for a white light coronagraph, where a Lyot Stop and occulters are needed to permit observations of faint coronal emissions when the solar disk is vastly brighter than the corona. The Ritchey-Chrétien is more compact than the aplanatic Gregorian for a given f/#, although the Petzval surface of the Ritchey-Chrétien has slightly greater curvature. For both types of two-mirror aplanatic telescopes, the field limit for good images is set by astigmatism. Since the image blur due to astigmatism is symmetric, it is possible to locate the centers of the images more accurately.

The Ritchey-Chrétien configuration was chosen for the Hubble telescope, and we also selected it for the MSSTA telescopes and this Lyman α Coronagraph/Polarimeter. Since the MSSTA instrument used no Lyot Stop or occulter, the Ly-α images obtained revealed the Ly-α coronal features simultaneously with the structures seen on the solar disk. These observations with the MSSTA f/28 Ritchey-Chrétien Ly-α coronagraph using ultrasmooth, flow-polished optics revealed that the solar corona out to 2 $R_\odot$ from disk center can be imaged simultaneously with spicules, loops, and threadlike structures on the limb and emission and absorption features on the disk.[19] These images were obtained using two relatively low transmission Acton VN Ly-α filters in conjunction ultrahigh resolution, but relatively insensitive, Kodak 649 photographic emulsions with extremely wide latitude. It is observed that the knowledge of the topological brightness distribution of the chromospheric illuminating source is very important to the interpretation of the coronal Ly-α data.[20] Contrary to the case of the infrared or optical forbidden lines in the corona, where the photospheric incident radiation field is virtually homogeneous (apart from a well-known limb darkening), the Ly-α chromospheric network is clearly visible. The network at Ly-α is easily seen in the MSSTA flight data and the presence of plage and active regions has to be considered.[18,20]

The modular instrument we are developing will be capable of measuring the linear polarization state of Ly-α line radiation. The Imager Module has been designed and ray traced using SYNOPSYS, OPTEC, and BEAM 4.[8] The results of the BEAM 4 analysis are shown in Figures 2-4. The on-axis and off-axis Modulation Transfer Function (MTF) for the 2.3-m focal length Ritchey-Chrétien at 1215.7 Å is shown in Figure 2. The MTF is 0.4 at 2000 cycles/mm on-axis, corresponding to a spatial resolution of $\sim$ 0.05 arc sec. At the edge of the field an MTF of 0.4 is at 200 cycles/mm (resolution $\sim$0.5 arc sec). Figure 3.a shows the Imager Module's on-axis geometrical blur spot diagram. The central peak is very sharp, subtending some 0.03 arc sec. The entire spot is 0.25 arc sec in diameter at the telescope plate scale of 11.15 μm/arc sec. In Figure 3.b, we present the phase map for the Ly-α Ritchey-Chrétien which reveals a central spot of 2.5μm diameter indicating a diffraction limited resolution of 0.22 arc sec. In Figure 4, we show (a) the two-dimensional spot diagram and (b) the three-dimensional point spread function of the LyαCoPo at the full field half angle of 0.7° which encompasses the disk and corona out to a heliocentric distance of 2.6 $R_\odot$.
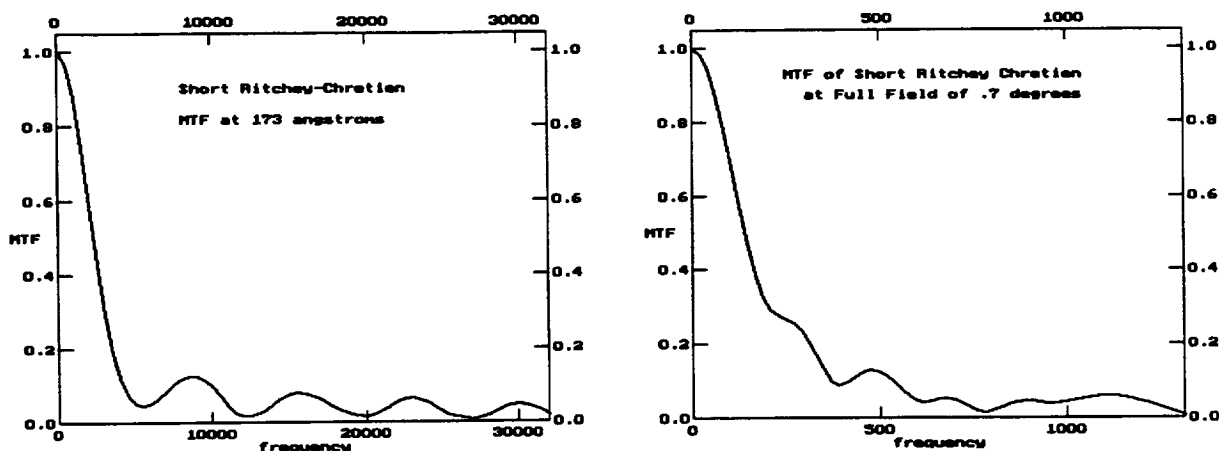
Figure 2. Results of ray trace analysis for the 2.3-m focal length Ritchey-Chrétien Imager Module for the All-Reflecting Lyman α Coronagraph/Polarimeter instrument showing the Modulation Transfer Function: (a) on-axis and (b) at 42 arc minutes off-axis.
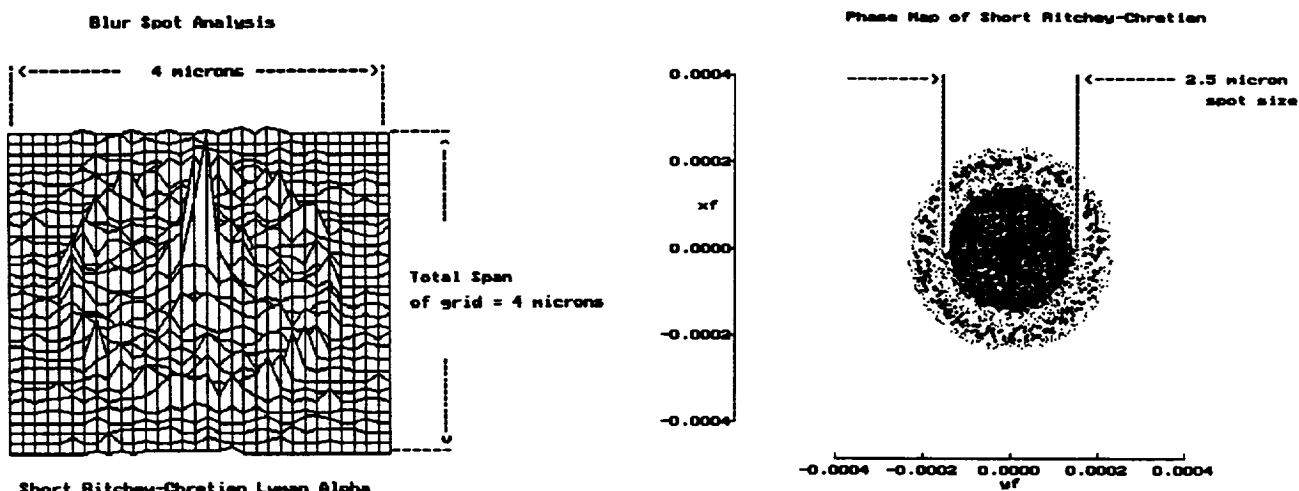

Figure 3. Ray trace calculation of (a) the on-axis three-dimensional geometrical blur spot diagram for the Lyman α Coronagraph/Polarimeter and (b) the diffraction phase map at 1215.7 Å. Spatial resolution of less than 0.25 arc sec is indicated by these results.

The LyαCoPo mirror substrates for the Imager Module are being fabricated of CVD silicon carbide using advanced flow polishing methods developed at Baker Consulting. These flow polishing methods, which permit accurate control of mid-range spatial frequency errors, have yielded 2 Å rms surfaces for the Zerodur optical components flown on the MSSTA and 0.5 Å rms surfaces for the hemlite grade Sapphire mirror substrates for the Water Window Imaging X-Ray Microscope.[21] Since the corona is much brighter relative to the disk at Ly-α than at visible wavelengths, the scattering and stray light reduction requirements are much less stringent for a Ly-α coronagraph than for a white light coronagraph. Indeed, based upon the results we achieved with the MSSTA Ly-α telescope, we are confident that the use ultrasmooth optics with multilayer polarizer and filter coatings make it possible to construct the LyαCoPo for coronal observations
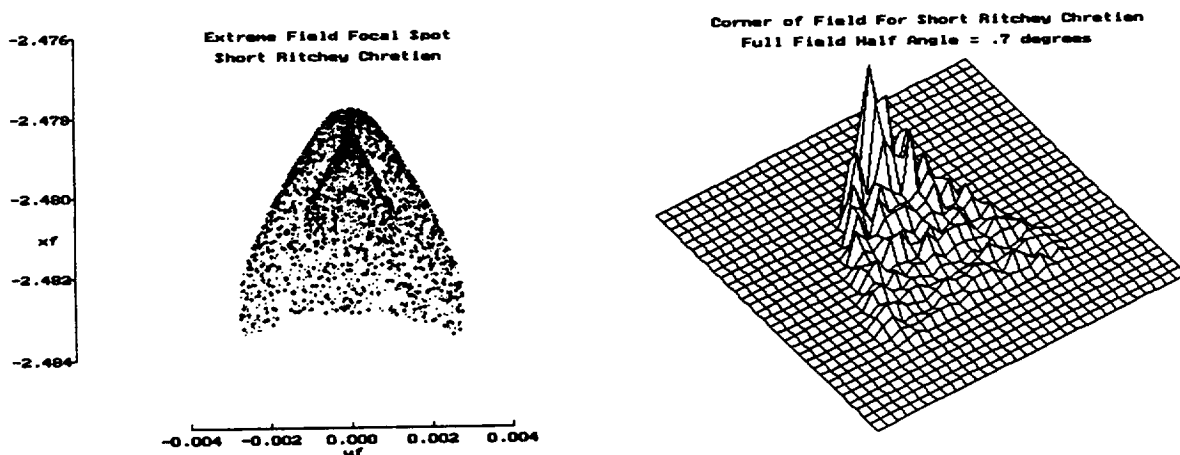
Figure 4. Ray trace results of imaging properties at the extreme edge of the field (42 arc min) for the 2.3-m focal length Ritchey-Chrétien Imager Module. Shown is (a) the two-dimensional spot diagram and (b) the three-dimensional point spread function.

without an occulter. Consequently, two of the optical configurations are designed to produce polarization analyzed images of the disk and corona simultaneously on the same film plane. The third configuration employs a "beam scraper" which is a type of inverse occulter. This system uses a polarizer mounted near the prime focus of the Ritchey-Chrétien Imager Module. This polarizer will be constructed with an elliptical aperture through which the disk image falls so as to minimize scattered radiation from the solar disk which is significantly brighter than the coronal image. This approach also permits the use of two photographic films simultaneously, which may be chosen with significantly differing spatial resolution and Ly-α sensitivity. Hence, very faint coronal features may be imaged simultaneously with the disk using similar exposure times without risking overexposure of the much brighter disk emission features. The elliptical aperture in the beam-scraper mirror allows the bright disk radiation into a light trap cavity thereby minimizing loss of contrast in faint, outer coronal features due to scattering of disk emission by imperfections or particulate contaminants on the polarizer and filter optical components.

We previously considered the Newtonian as well as the Ritchey-Chrétien optical configuration in optical systems using Brewster angle polarization analyzers [8] coupled with Acton Research Ly-α transmission filters. However, exctiting results have recently been achieved at UAH with dielectric multilayer thin film FUV polarizers based upon the principles of induced transmission and absorption, which were pioneered by Berning and Turner.[22] In 1957, they observed that a thick metal film can be induced to transmit a very large amount of energy at a specific wavelength when it is surrounded by the proper interference film combination. They employed this principle to design narrow bandpass filters. This principle forms the basis for the thin film induced transmission and absorption polarizers, which are far superior to Brewster angle polarizers for use at Ly-α. They can be made to operate at 45°, which is ideal for the optical configurations we have chosen. In addition, the induced transmission and absorption coatings offer very high reflectivities at 1215.7 Å and vastly superior s/p ratios than is possible with conventional Brewster angle polarization analyzers. Since their response remains constant over a wide range of angles of incidence (Fig. 5), they are well suited for non-telecentric systems. As for the induced transmission and absorption Ly-α filters, they offer significantly higher transmission and narrower bandpass at Ly-α than can be achieved with the Acton transmission filters as were used for MSSTA.

Kim et al.[15] have recently investigated polarizers and filters using two layers of MgF_2 as the low absorbing material and a thick central layer of Al as the high absorbing material. The top MgF_2 layer serves as the

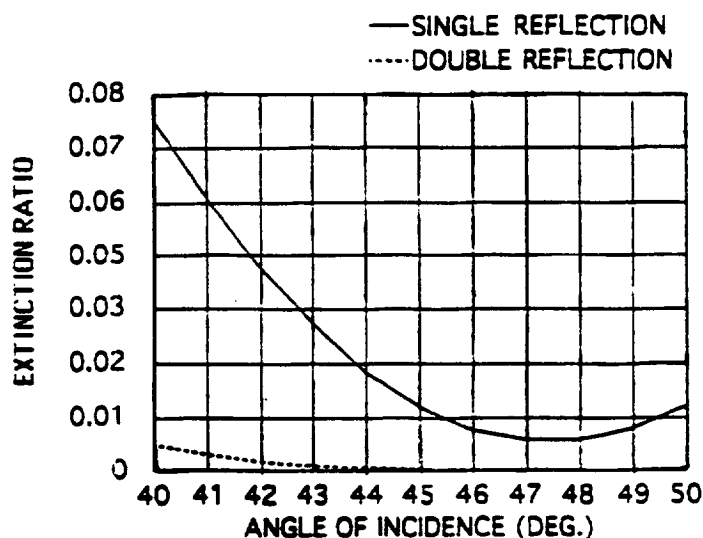—SINGLE REFLECTION
----DOUBLE REFLECTION

Figure 5. Polarization extinction ratio ($ER \equiv p/s$) as a function of the angle of incidence (from 40° to 50°) for a thin-film polarizer designed to operate at 45°. The beam angular divergence due to the f-number of the telescope is about ±1.5° from the chief ray direction. The extintion ratio variation caused by this divergence is $\Delta ER \lesssim 0.01$, corresponding to a fractional error in polarization measurements of $\Delta P/P \lesssim 1\%$.

transmission induced layer for the p-polarization state and the bottom MgF_2 layer acts as a transmission and absorption induced layer. There are large differences in the Fresnel transmission and reflection coefficients for these two layers. Consequently, they work differently for the s-polarization state, thus a high degree of polarization can be achieved. It has been computed that a single Ly-α polarizer operating at 45° can achieve 88.67% reflectance for the s-polarization state and 1.21% for the p-polarization state, yielding a 97.3% degree of polarization (Fig. 6). With two polarizers a 99.96% degree of polarization can be realized while the throughput for the s-polarized radiation is 78.6%. These characteristics make it possible to construct, for the first time, Ly-α polarizers with a high throughput combined with a very high polarization efficiency. Due to the reasonably large degree of polarization ($\gtrsim 10\%$) in the neutral hydrogen Ly-α flux from the solar corona, this affords a very adequate level of polarization analysis. Hence, all-reflecting Ly-α systems can employ double polarizers and filters to yield far higher throughput and narrower bandpass at Ly-α than a single Brewster angle polarizer with a single Acton VN transmission filter as we previously described.

The exceptionally high reflectances afforded by these new optics have led us to conclude that there is there is no longer a need to consider the Newtonian configurations which minimize the number of reflections required, but offer much poorer optical performance over the wide fields of view needed for observations of the outer corona. Indeed, we can take advantage of the far better off-axis performance afforded by Ritchey-Chrétien systems. An all-reflecting Ritchey-Chrétien LyαCoPo system offers simplicity and excellent resolution over wide field angles. Furthermore, it does not require the use of Ly-α refractive elements which could introduce undesired phase shifts and retardances. We note that theoretical studies by Kim et al.[16] indicate that their coating techniques and methods should allow the production Ly-α retarders for use in instruments capable of measuring circular polarization of Ly-α radiation, which could yield information about macroscopic electrostatic fields in the low corona.[23]

The LyαCoPo configurations we are developing are shown in Figs. 7-8. The simplest configuration, which uses a single induced transmission and absorption polarizer and filter to deliver maximum throughput, is shown in Fig. 7a. This system requires films with low visible light sensitivity such as the KODAK 649 or the Agfa 10E75 emulsions. Figure 7b. shows the system with two reflecting induced transmission and absorption polarizers and two Ly-α filters. This configuration yields excellent visible light suppression and notably higher s/p ratios. It may yield even higher sensitivity, as it can be used with films that have
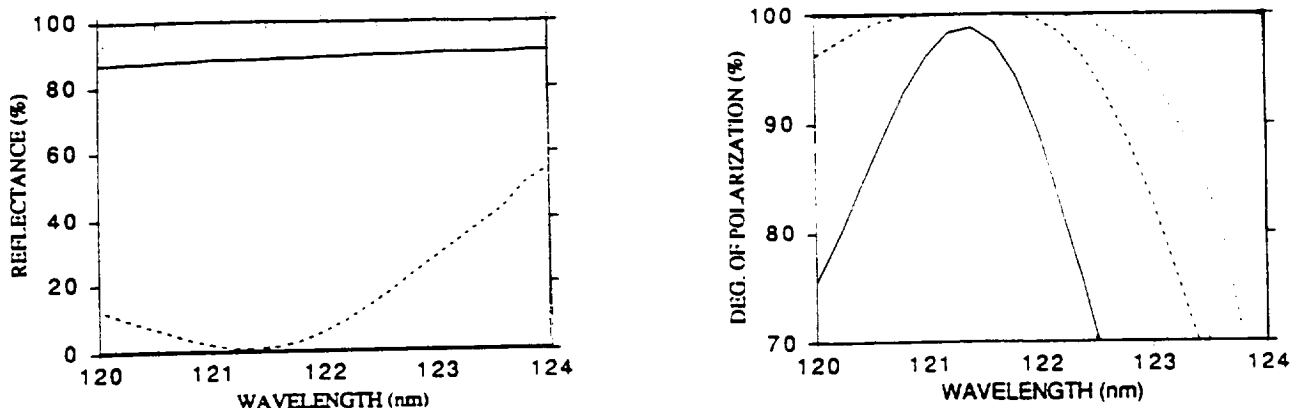
Figure 6a. Calculated reflectances for s-polarization (solid line) and p-polarization (dashed line) for a Ly-α polarizer at 45° angle of incidence. (b) Degree of polarization as a function of wavelength λ around Ly-α for single (solid line), double (dashed line), and (dotted line) reflection polarizer made of the design of Fig. 6.a.
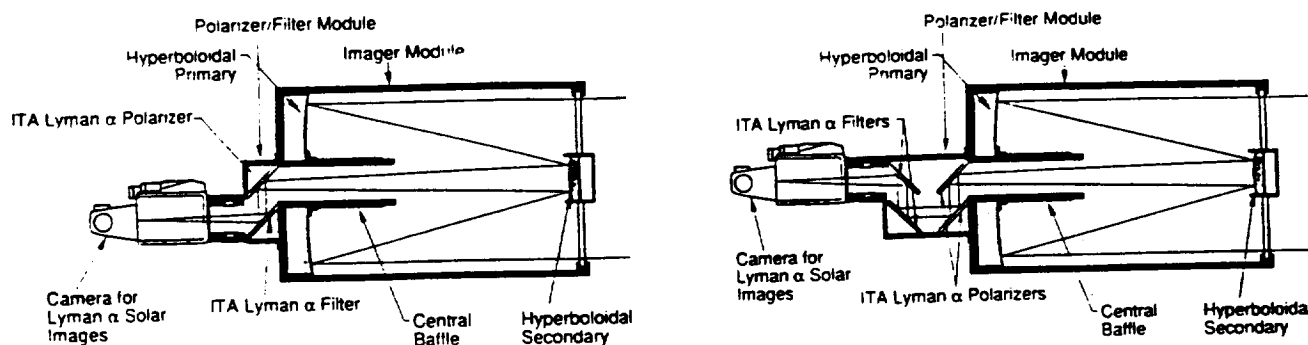

Figure 7. Schematic layout of the all-reflecting Ritchey-Chrétien coronagraph/polarimeter using (a) single Ly-α induced transmission and absorption (ITA) polarizer followed by the Ly-α reflecting ITA filter, and (b) two Ly-α ITA polarizers and filters. With this double polarizer/double filter system, much better visible light rejection and higher s/p ratio is achieved the expense of a slight loss of throughput.

somewhat higher sensitivity to visible light and Ly-α than 649. Our synchrotron studies indicate that the Agfa 10E56 and 8E56 films have much higher sensitivity to 1215.7-Å radiation than the 649 emulsion, while exhibiting only slightly higher visible light sensitivity.[24,25] However, they afford much higher spatial resolution (5000 li/mm) than 649 (2000 li/mm). Figure 8 shows the Ly-α Coronagraph/Polarimeter system with the "beam scraper" configuration. It should be noted that even though the system has a physical appearance similar to the configuration with the double polarizer and double filter shown in Fig. 7b, the optical properties are like that of the single system, in that each component of the image encounters only a single polarizer and a single filter. Although we will conduct both theoretical and experimental studies of this configuration, at the present time we believe the system shown in Figure 7b represents the instrumental configuration which will yield the highest optical performance.
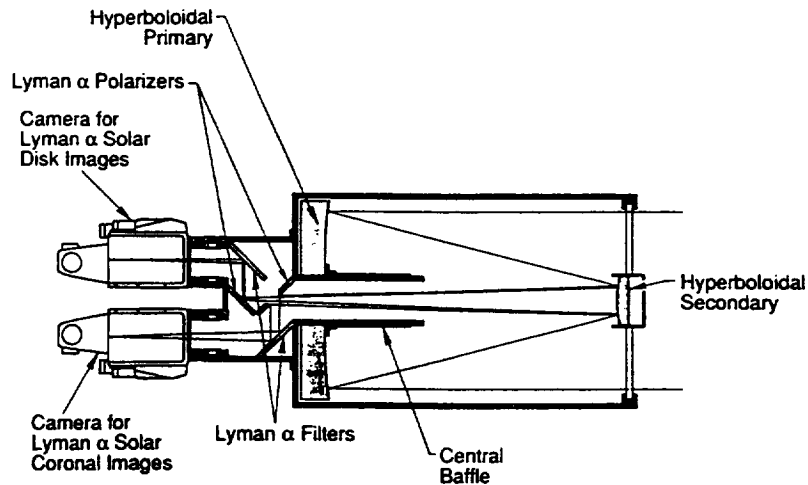
Figure 8. Schematic layout of the all-reflecting coronagraph/polarimeter with the "beam-scraper" optical system. The light from the bright solar disk falls throught the elliptical aperture in the polarizer optic into the light trap cavity. Two cameras may be used such that the disk and coronal images are recorded simultaneously of different film types.

The theoretical studies which we have carried out to date have revealed the original MSSTA Ritchey-Chrétiens capable of providing spatial resolution of the order of 0.3 arc sec out to 10 arc min off-axis. Hoover et al.[26] have measured the MSSTA Ritchey-Chrétien telescopes and photographically demonstrated visible light performance of 0.5 arc sec over the entire 48 arc min (unvignetted) field of view. The field limit for high resolution images from aplanatic telescopes is constrained by astigmatism and field curvature. The MSSTA telescopes are diffraction limited over the entire field of view.

For the LyαCoPo Imager Module, we have performed preliminary designs of a 2.3-m focal length Ritchey-Chrétien using SYNOPSYS. The primary/secondary separation was 0.54 m for an f/18 system which has an unvignetted FOV out to $r = 3$ R$_\odot$ and much higher throughput than the MSSTA Ly-α Ritchey-Chrétien. Hoover et al.[8] have reported the results of a diffraction image analysis of the MSSTA and the LyαCoPo. The LyαCoPo design offers a considerable improvement in angular resolution over the MSSTA telescopes. The aplanatic LyαCoPo we have examined has the advantage that optimal placement of the polarization analyzer is possible as it can be situated very close to the prime focus. Since this is an aplanat, the primary image degradation arises from curvature of field and astigmatism. At the edge of the usable field of aplanatic telescopes, the distortion is usually only a few hundredths of an arc second. Matching the Petzval surface is impractical with photographic systems where film transport is desired. Balanced resolution over the entire field is possible by placing the film plane so as to transect the surface of best focus.[8] By moving the flat detector plane toward the MSSTA primary by 0.04 cm it is possible for the resolution to remain better than the 0.5 arc sec range over a full 50 arc min full field of view which would allow ultra-high resolution observations of the inner corona. Since most prior coronagraphs had spatial resolution ∼ 8 arc sec, this represents a vast improvement.

5. POLARIZATION ANALYSIS TECHNIQUES

The polarization analysis can be accomplished by rotating the polarizer or telescope, but it is not required that rotating optics be employed. Indeed, the measurement of the state of polarization could be accomplished by rolling the rocket between successive observations. Indeed, the Stokes parameters can be obtained directly by taking successive images with the rocket oriented, for instance, at 0°, 45°, 90° and 135° of roll. (In principle, only three orientations would be required to recover the three Stokes parameters of interest; the fourth additional orientation, however, allows useful redundancy in the data.) It is not essential that the roll angles be precise as long as the exact roll angle achieved in flight is well known. This information is contained in the solar images to high accuracy. By processing all images simultaneously in a well-controlled

development system, the polarization measurements can be made from digitized images. Accurate FUV calibration of the film is possible if pre-exposed calibration strips are spliced onto the flight film. Processing calibration strips with the flight film and digitizing them with the flight images would facilitate the accurate conversion of density values measured by a microdensitometer into quantitative representations of the solar flux intensities. The Stokes parameters for the linear polarization, $\langle S_i \rangle$; $i = 0, 1, 2$ (see Ref. 18), could then be obtained directly by the sums and differences of the signal, $S(\rho)$, in the images recorded at the different roll angles, ρ, since:

$$\langle S_0 \rangle = [S(0°) + S(90°)], \quad \langle S_1 \rangle = [S(0°) - S(90°)], \quad \text{and} \quad \langle S_2 \rangle = [S(45°) - S(135°)]. \tag{1}$$

These images would be sequentially recorded so the polarization measurements are not precisely simultaneous. If absolute simultaneity were required, three precisely calibrated polarimeters oriented, for instance, at -60°, 0°, and +60°, could be used. However, we do not anticipate that significant changes in the polarization state in the large coronal structures would occur on time scales as short as tens of seconds, such as would be available for recording the images from a sounding rocket flight.

6. IMAGE RECORDING TECHNIQUES

Due to the desire to record disk features simultaneously with coronal images with excellent spatial resolution (0.1 - 1 arc sec) over a wide field of view, the optimal recording medium is ultrahigh resolution, wide latitude photographic film in 70-mm format. During the MSSTA program, we tested many EUV/FUV films; tabular grain XUV sensitive emulsions, Schumann and spectroscopic emulsions. For the MSSTA flight we used the high sensitivity, moderate resolution XUV 100 film for recording faint solar features. This film was ultrasonically spliced to the slightly lower sensitivity 649 film, which was used to obtain high resolution soft x-ray/EUV/FUV images of the Sun. We established that, by processing the wide latitude 649 film in Dektol, its sensitivity can be enhanced to the extent that it can be used for producing high resolution images of faint far coronal features simultaneously with bright loops and active regions. Consequently, structural features on the disk and in the inner corona can be observed with high resolution and good contrast while the much fainter outer coronal features are also recorded for subsequent analysis by computer imaging techniques.[24] During the past year, we have tested several films at the NIST SURF II synchrotron and found that Agfa 10E75 emulsion is 1 to 2 orders of magnitude more sensitive than the 649 film at EUV and FUV wavelengths and affords much higher resolution and greater dynamic range.[25]

Fineschi et al.[18] have shown that, for meaningful diagnostics of coronal magnetic fields via the Hanle effect, a signal-to-noise ratio of $\gtrsim 70$ is required. As an imaging detector, we plan to use 70-mm photographic films. The photographic signal-to-noise can be expressed in the following way[27,28]

$$S/\Delta S = 0.4343 \cdot \gamma / \sqrt{D \cdot (A_{grain}/A_{pixel})}, \tag{2}$$

where γ is the slope of the characteristic curve, D the photographic diffuse density, and A_{grain} and A_{pixel} are the grain and the pixel area, respectively. The Ly-α sensitive 10E75 emulsion has grain size $\lesssim 0.3$ μm and can be processed to achieve $\gamma \geq 2$. Diffuse densities $D \sim 1$ can be obtained for proper exposures of the inner Ly-α corona. The fast microdensitometer at the Sacramento Peak Obsercatory that we use for film digitization examines ~ 30 μm pixels on enlarged, high resolution, first generation internegatives. With the above values inserted in Eq. (2), it is clear that the requirement of a signal-to-noise ~ 70 can be fulfilled.

7. OBSERVATIONAL CONSIDERATIONS WITH THE LyαCoPo

Interpretation of measurements of Ly-α coronal emission must take into account the effect of geocoronal absorption/emission. Since the polarimetric observations we plan for this instrument are in the near corona ($r < 2$ $R_\odot$), the effects of the geocoronal absorption are more important than those due to the geocoronal emission.[29] However, the geocoronal absorption feature is much narrower (FWHM ~ 0.03 Å) than the profile of the solar line (FWHM ~ 1 Å).[30] Therefore, when the line is viewed in integrated profile, as we plan to do, the reduction in intensity due to geocorona is relatively limited. The instrument bandpass is determined by

the optical coatings and the filter transmission. Mirror coatings currently have bandpasses of the order of $30 - 60$ Å, although methods are being explored for producing Ly-α systems with overall bandpass throughput which is significantly narrower.[31]

A signal (from coronal radiation) to noise (stray light) ratio $\gtrsim 10$ is required for meaningful polarimetric measurements of the Ly-α Hanle effect.[18] This corresponds to a stray light rejection requirement of 10^{-5} to 10^{-6} for observations of the coronal Lyman α radiation out to r ~ 2 $R_\odot$. This requirement can be achieved with the utilization of optical surfaces with rms smoothness of ≤ 2 Å, strenuous contamination control, and a central baffle for the interior of the telescope primary mirror. Furthermore, the noise originating from the stray light can be extracted by performing the polarization analysis. The stray light is expected to be unpolarized and, therefore, by taking the difference of the intensity measurements for different positions of the polarizer, the signals due to scattered light will cancel out. Finally, the Ly-α filter used in the camera system and the low visible light sensitivity of the film achieves the necessary suppression of the off-band photospheric visible light and UV emission. The problem of the influence of both geocorona and stray light on the Ly-α polarimetric mesureaments is discussed in more detail in another paper of this volume.[18]

8. CORRELATIVE OBSERVATIONS

In analyzing the results from the LyαCoPo, it will be useful to utilize correlative solar observations. The observed integrated intensity is proportional to the number of protons along the line of sight – or equivalently, the number of electrons. Thus correlative measurements of the line-of-sight electron density over the same spatial regions as observed by the LyαCoPo serve as an additional "calibration" of the integrated intensity. Limb data from the K-Coronameter observations would serve this purpose well. Observations from the High Altitude Observatory K-Coronameter may be correlated with the LyαCoPo observations. Furthermore, polarization observations of visible forbidden lines (e.g., green line) from the Sacramento Peak Coronagraph could also yield additional information on the direction of coronal magnetic fields.[32] In addition, observations of the surface vector magnetic fields obtained with the MSFC vector magnetograph or the HAO Advanced Stokes Polarimeter could be utilized to establish the lower boundary condition for the coronal magnetic field, and form a basis for comparison of magnetic field extrapolations with our results. These observations may be scheduled in concert with flights of the LyαCoPo. Additionally, depending upon which instruments are available when the LyαCoPo instrumentation obtains a flight opportunity, valuable correlative observations may be obtained with the grazing incidence x-ray imaging telescope on the YOKOH satellite, the UVCS instrument aboard SoHO, and the XUV instruments aboard the Russian Coronas I spacecraft. The LyαCoPo instrument may ultimately be flown on the shuttle, a Small Explorer Satellite or Space Station. This would provide the long observing times desired to perform (i) indepth investigations of coronal transient phenomena, and (ii) synoptic studies of long-term evolution of three-dimensional structures in the corona.

9. CONCLUSIONS

We are developing an All-Reflecting Lyman-α Coronagraph/Polarimeter (LyαCoPo) for diagnostics of coronal vector magnetic fields by observations of the Hanle effect on the Ly-α (1215.7 Å) coronal line, which is linearly polarized by resonance scattering from neutral hydrogen atoms in the solar corona. This new instrument comprises a 2.3-m focal length Ritchey-Chrétien telescope, reflecting polarizers and narrow bandpass filters operating at 45°. It uses ultrasmooth optics without an occulter so as to permit the Ly-α chromospheric excitation source on the solar disk to be observed simultaneously with measurements of the structure and polarization characteristics of the Ly-α corona. Theoretical ray trace analysis has revealed the optical system to have diffraction-limited performance, with spatial resolution better than 0.25 arc sec. The LyαCoPo incorporates advanced induced transmission and absorption Ly-α polarizers and filters, which combine high throughput at Ly-α with high polarization efficiency. These new polarizers have polarization characteristics which are relatively insensitive to small variations from the design angle of incidence, and hence they are well suited for non-telecentric applications. The LyαCoPo instrument can be utilized with high sensitivity, wide dynamic range 70-mm photographic films for solar coronal observations out to 4 $R_\odot$. Observations with this All-Reflecting Ly-α Coronagraph/Polarimeter, combined with knowledge of the Hanle effect, could yield the first direct diagnostics of the strength and direction of magnetic fields (i.e., assessments of vector magnetic fields) in the solar corona.

10. ACKNOWLEDGEMENTS

11. REFERENCES

1. Arthur B. C. Walker, Jr., Troy W. Barbee, Jr., Richard B. Hoover, and Joakim F. Lindblom, "Soft X-Ray Images of the Solar Corona with a Normal Incidence Cassegrain Multilayer Telescope," *Science*, **241**, 1781-1787 (1988).

2. Arthur B. C. Walker, Jr., Troy W. Barbee, Jr., Richard B. Hoover, and Joakim F. Lindblom, "Monochromatic X-Ray and XUV Imaging with Multilayer Optics," *J. de Physiques Colloques*, **C1 49**, C1-175 (1988).

3. Arthur B. C. Walker, Jr., Richard B. Hoover, J. F. Lindblom, R. H. O'Neal, M. J. Allen, and T. W. Barbee, Jr., "Astronomical Observations with Normal Incidence Multilayer Optics," *Physica Scripta*, **41**, 1035-1062 (1990).

4. Arthur B. C. Walker, Jr., Richard B. Hoover, and Troy W. Barbee, Jr., "Chromospheric and Coronal Observations with Multilayer Optics," in *Multilayer and Grazing Incidence X-Ray/EUV Optics for Astronomy and Projection Lithography*, Richard B. Hoover and Arthur B. C. Walker, Jr., eds., *Proc. SPIE*, **1742** (1992), this volume.

5. Arthur B. C. Walker, Jr., Richard B. Hoover, and Troy W. Barbee, Jr., "High Resolution Thermally Differentiated Images of the Chromosphere and Corona," in *Advances in Stellar and Solar Coronal Physics*, Jeffrey L. Linsky, ed. (1992), in press.

6. Phillip C. Baker, "Advanced Flow-Polishing of Exotic Optical Materials," in *X-Ray/EUV Optics for Astronomy, and Microscopy*, R. B. Hoover, ed., *Proc. SPIE*, **1160**, 263-270 (1989).

7. Phillip C. Baker and Richard B. Hoover, "Metrology of X-Ray Optics Utilizing Shearing Interferometric Techniques," in *Multilayer and Grazing Incidence X-Ray/EUV Optics*, Richard B. Hoover and Arthur B. C. Walker, Jr., eds., *Proc. SPIE*, **1546**, 137-149 (1992).

8. Richard B. Hoover, Silvano Fineschi, Arthur B. C. Walker, Jr., R. Barry Johnson, and M. Zukic, "Optical Configurations for H I Lyman α Coronagraph/Polarimeters," in *Multilayer and Grazing Incidence X-Ray/EUV Optics*, R. B. Hoover and A. B. C. Walker, Jr., eds., *Proc. SPIE*, **1546**, 414-431 (1992).

9. Richard B. Hoover, Arthur B. C. Walker, Jr., C. DeForest, M. J. Allen, J. F. Lindblom, C. A. Dewan, L. Gilliam, T. Brown, and L. November, "Photographic Films for the Multi-Spectral Solar Telescope Array," in *Multilayer and Grazing Incidence X-Ray/EUV Optics*, Richard B. Hoover and Arthur B. C. Walker, Jr., eds., *Proc. SPIE*, **1546**, 188-204 (1992).

10. Robert M. MacQueen, J. Gosling, E. Hildner, R. Munro, A. Poland, and C. Ross, "The High Altitude Observatory White Light Coronagraph," in *Instrumentation in Astronomy II, Proc. SPIE*, **44**, 207 (1974).

11. Robert M. MacQueen, A. Csoeke-Poeckh, E. Hildner, L. House, R. Reynolds, A. Stanger, H. Tepoel, and W. Wagner, "The High Altitude Observatory Coronagraph/Polarimeter on the Solar Maximum Mission," *Solar Phys.*, **65**, 91 (1980).

12. Silvano Fineschi, Richard B. Hoover, Juan M. Fontenla, and Arthur B. C. Walker, Jr., "Polarimetry of Extreme Ultraviolet Lines in Solar Astronomy, "*Optical Engineering*, **30**, 1161 (1991).

13. R. M. Bonnet, E. C. Bruner, L. W. Acton, W. A. Brown, and M. Decaudin, "High-Resolution Lyman-α Filtergrams of the Sun," *Ap. J. Lett.*, **237**, L47 (1980).

14. Richard B. Hoover, Phillip C. Baker, James Hadaway, R. B. Johnson, C. Peterson, D. R. Gabardi, J. F. Lindblom, and Arthur B. C. Walker, Jr., "Performance of the Multi-Spectral Solar Telescope Array III, Optical Characteristics of the Ritchey-Chrétien and Cassegrain Telescopes," in *X-Ray/EUV Optics for Astronomy and Microscopy*, Richard B. Hoover, ed., *Proc. SPIE*, **1343**, 404-414 (1991).

15. J. Kim, M. Zukic, and D. G. Torr, "Multilayer Thin-Film Designs as Far-UV Polarizers," in *Multilayer and Grazing Incidence X-Ray/EUV Optics for Astronomy and Projection Lithography*, Richard B. Hoover and Arthur B. C. Walker, Jr., eds., *Proc. SPIE*, **1742** (1992), this volume.

16. J. Kim, M. Zukic, D. G. Torr, and M. M. Wilson, "Multilayer Thin Film Designs as Far-UV Qaurterwave Retarders," in *Multilayer and Grazing Incidence X-Ray/EUV Optics for Astronomy and Projection Lithography*, Richard B. Hoover and A. B. C. Walker, Jr., eds., *Proc. SPIE*, **1742** (1992), this volume.

17. M. Born, and E. Wolf, *Principles of Optics*, Pergamon Press, 6th ed., 1980, p. 187.

18. Silvano Fineschi, Richard B. Hoover, M. Zukic, J. Kim, Arthur B. C. Walker, Jr., R. Barry Johnson, and Phillip C. Baker, "Polarimetry of H I Lyman α for Coronal Magnetic Field Diagnostics," in *Multilayer and Grazing Incidence X-Ray/EUV Optics for Astronomy and Projection Lithography*, Richard B. Hoover and Arthur B. C. Walker, Jr., eds., *Proc. SPIE*, **1742** (1992), this volume.

19. Richard B. Hoover, A. B. C. Walker, Jr., J. F. Lindblom, M. J. Allen, R, ONeal, and C. DeForest, "Solar Observations with the Multi-Spectral Solar Telescope Array," in *Multilayer and Grazing Incidence X-Ray/EUV Optics*, R. B. Hoover and A. B. C. Walker, Jr., eds., *Proc. SPIE*, **1546**, 175-187 (1992).

20. S. Fineschi, R.B. Hoover, and A.B.C. Walker Jr., "Hydrogen Lyman α Coronagraph/Polarimeter," in *Multilayer and Grazing Incidence X-Ray/EUV Optics*, R. B. Hoover, ed., *Proc. SPIE*, **1546**, 402 (1992).

21. Richard B. Hoover, David L. Shealy, A. B. C. Walker, Jr., and P. C. Baker, "Development of the Water Window Imaging X-Ray Microscope," in *Multilayer and Grazing Incidence X-Ray/EUV Optics*, Richard B. Hoover and Arthur B. C. Walker, Jr., eds., *Proc. SPIE*, **1546** 125-136, (1992).

22. P. H. Berning, and A. F. Turner, "Induced Transmission in Absorbing Films Applied to Band Pass Filter Design," *J. Opt. Soc. Am.*, **47**, 230 (1957).

23. B. Favati, E. Landi Degl'Innocenti, and M. Landolfi, "Resonance Scattering of Lyman-α in the Presence of an Electrostatic Field," *Astron. Astrophys.*, **179**, 329 (1987).

24. R. B. Hoover, C. DeForest, J. F. Lindblom R. H. O'Neal, C. Peterson, A. B. C. Walker, Jr., and A. DeWan, "EUV/FUV Response Characteristics of Photographic Films for the Multi-Spectral Solar Telescope Array," *Optical Engineering*, **30**, 1116-1124, (1991).

25. Richard B. Hoover, Arthur B. C. Walker, Jr., Craig DeForest, R. N. Watts and C. Tarrio, " Ultrahigh Resolution Photographic Films for X-Ray/EUV/FUV Astronomy," in *Multilayer and Grazing Incidence X-Ray/EUV Optics for Astronomy and Projection Lithography*, Richard B. Hoover and Arthur B. C. Walker, Jr., eds., *Proc. SPIE*, **1742** (1992), this volume.

26. R. B. Hoover, T. W. Barbee, Jr., P. C. Baker, J. F. Lindblom, M. Allen, C. DeForest, C. Kankelborg, R. O'Neal, E. Paris, and A. B. C. Walker, Jr., "Performance of Compact Multilayer Coated Telescopes at Soft X-Ray, EUV, and VUV Wavelengths, " *Optical Engineering*, **29**, 1281 (1990).

27. H. C. Andrews and B. R. Hunt, *Digital Image Restoration*, Prentice-Hall, New Jersey, (1977).

28. I. Furenlid, W. E. Schoenog, and B. E. Carder Jr., "A Method for Determining Photographic Signal-to-Noise," *AAS Photo-Bulletin*, **16**, 14 (1977).

29. Jaques M. Beckers, and Eric Chipman, "The Profile and Polarization of the Coronal Ly-α Line," *Solar Phys.*, **34**, 151 (1974).

30. R. R. Meier and D. K. Prinz, "Absorption of the Solar Lyman Alpha Line by Geocoronal Atomic Hydrogen," *J. Geophys. Res.*, **75**, 6969 (1970).

31. Muamer Zukic, Douglas G. Torr, James F. Spann, and Marsha R. Torr, "Vacuum Ultraviolet Thin Films. 2: Vacuum Ultraviolet All-Dielectric Narrowband Filters," *Applied Opt.*, **29**, 4293 (1990).

32. Charles W. Querfield, and Raymond N. Smartt, "Comparison of Coronal Emission-line Structure and Polarization," *Solar Phys.*, **91**, 299 (1984).